Computation of excited states for the nonlinear Schrödinger equation: numerical and theoretical analysis

Christophe Besse, Romain Duboscq, Stefan Le Coz

COMPUTATION OF EXCITED STATES FOR THE NONLINEAR SCHRÖDINGER EQUATION: NUMERICAL AND THEORETICAL ANALYSIS

CHRISTOPHE BESSE, ROMAIN DUBOSCQ, AND STEFAN LE COZ

Abstract. Our goal is to compute excited states for the nonlinear Schrödinger equation in the radial setting. We introduce a new technique based on the Nehari manifold approach and give a comparison with the classical shooting method. We observe that the Nehari method allows to accurately compute excited states on large domains but is relatively slow compared to the shooting method.

1. Introduction

We consider the nonlinear Schrödinger equation

$$iu_t + \Delta u + f(u) = 0 \tag{1}$$

where $u : \mathbb{R} \times \mathbb{R}^d \to \mathbb{C}$ and $f \in \mathcal{C}^1(\mathbb{R}, \mathbb{R})$ is an odd function extended to $\mathbb{C}$ by setting $f(z) = f(|z|)z/|z|$ for all $z \in \mathbb{C} \setminus \{0\}$. Equation (1) arises in various physical contexts, for example in nonlinear optics or in the modelling of Bose-Einstein condensates. For physical applications as well as for its numerous interesting mathematical properties, (1) has been the subject of an intensive research over the past forty years. We refer for example to the books of Cazenave [12], Fibich [17] and Sulem and Sulem [24] for an overview of the known properties of (1) and references.

In this paper, we focus on special solutions of (1), the so-called *standing waves*. They are solutions of the form $e^{i\omega t}\phi(x)$ with $\omega > 0$ and ϕ satisfying

$$\begin{cases} -\Delta\phi + \omega\phi - f(\phi) = 0, \\ \phi \in H^1(\mathbb{R}^d) \setminus \{0\}. \end{cases} \tag{2}$$

Among solutions of (2), it is common to distinguish between the *ground states*, or *least energy solutions*, and the other solutions, the *excited states*. A *ground state* is a solution of (2) minimizing among all solutions of (2) the functional S, often called *action*, defined for $v \in H^1(\mathbb{R}^d)$ by

$$S(v) := \frac{1}{2}\|\nabla v\|_{L^2}^2 + \frac{\omega}{2}\|v\|_{L^2}^2 - \int_{\mathbb{R}^d} F(v)dx, \tag{3}$$

where $F(z) := \int_0^{|z|} f(s)ds$ for all $z \in \mathbb{C}$. An *excited state* is a solution of (2) which is *not* a ground state. In general, we shall refer to any solution of (2) as *bound*

Date: July 5, 2023.

2010 *Mathematics Subject Classification.* 35Q55,35C08,65N06.

Key words and phrases. Nonlinear Schrödinger Equation; Excited States; Numerical Method; Nehari Manifold.

This work was supported by the ANR LabEx CIMI (grant ANR-11-LABX-0040) within the French State Programme "Investissements d'Avenir".

state. Sufficient and almost necessary hypotheses on f to ensure the existence of bound states are known since the fundamental works of Berestycki and Lions [7, 8] and Berestycki, Gallouët and Kavian [6]. Under these hypotheses, it is proved in [6, 7, 8] that, except in dimension $d = 1$ where all bound states are ground states, there exist ground states and infinitely many excited states.

Note that the terminology *ground state* may be understood in different ways depending on the context. Some authors may call ground state any minimizer of the energy functional under the mass constraint. For power-type mass-subcritical nonlinear Schrödinger equations, this definition will coincide with ours, However, in other settings such as for the power-type mass-supercritical nonlinear Schrödinger equations, the two definitions do not coincide any more (there is no ground states in the later sense).

With our definition of ground states, it has long been established for power-type nonlinearities that ground states are positive, radial, and unique (see [19, 20]). On the other hand, excited states will necessarily change sign, and may even be complex valued (see e.g. [21]). They also need not to be radial, nor to even have any kind of symmetry group (as was shown recently in [3]).

There are numerous works devoted to the numerical calculations of ground states. Among many others, we find the seminal work of Bao and Du [4] devoted to the gradient flow with discrete normalisation which has been used in many settings (including by the authors of the present paper in the context of quantum graphs [9, 10]). We also mention the work of Choi and McKenna [13] devoted to the numerical implementation of the Mountain Pass approach, which has also been followed by numerous extension and improvements (see e.g. [22]). The Mountain Pass approach can be modified to compute nodal states, as was done by Costa, Ding and Neuberger [16], whose approach was later followed by Bonheure, Bouchez, Grumiau, and van Schaftingen [11]. Not many other works in the literature are devoted to the calculation of excited states, and to our knowledge this paper is the first one to present an approach based on the Nehari manifold.

Our goal in this article is to develop numerical methods for the computation of excited states. We will also take this opportunity to study numerically some properties of the excited states and establish some conjectures that could be further investigated theoretically.

The two methods that we are considering are the *shooting method* and the *Nehari method*. The *shooting method* is a classical method for the computation of solutions of boundary value problems. It consists in transforming the d-dimensional partial differential equation into an ordinary differential equation by considering radial solutions. The boundary value problem for the ordinary differential equation is then converted into an initial value problem, which can be easily solved using a standard scheme such as the Runge-Kutta 4th order method. In the present case, since we are working with an elliptic problem, we are led to consider initial conditions on the solution and its first derivative. The first derivative is necessarily set to 0 since its originating from a smooth radial function. We are thus left with the initial value of the solution which will be used as a parameter to be chosen in order to recover the boundary condition at infinity. The method is described in Section 3.

The idea of the *Nehari method* originates from the variational characterization of bound states as minimizers of the action functional under constraints build upon the Nehari functional. In the case of the ground state, we simply minimize the action

among functions for which the Nehari functional vanishes. To obtain excited states more elaborate constructions are required. For example, one may minimize the action on functions having non-trivial positive and negative parts both satisfying the Nehari constraint. We establish the existence of a solution (called *least energy nodal minimizer*) to this variational problem in a radial setting in Theorem 2.3. We refer to Section 2 for more details on the theoretical background. The numerical approach is based on a projected gradient method which consist in one step of gradient flow for the action followed by a projection on the chosen space of constraints. The method is described in Section 4. While being a standard theoretical tool, the Nehari approach has been seldom used in numerical analysis. To our knowledge, this paper is the first to investigate the computation of excited states using a Nehari approach.

While the shooting method is the go-to method for finding excited states, we identified some limitations of this approach. Indeed, it can only compute radial excited states, while the Nehari method could be extended to non-radial problems. Moreover, even in the radial case, the length of the interval on which the solution is computed is limited for the shooting method due to propagation of the error from the initial condition. This issue is not present for the Nehari approach. On the other hand, the convergence of the Nehari approach is much slower compared to the shooting method which has a maximal number of iteration for a given precision. The two methods are discussed in Section 5.

We conclude this paper by some numerical experiments. We investigate numerically the relation between the initial values of the bound states and their total number of nodes. We also study the positions of the nodes and the extremal values between two consecutive nodes. For each case, we provide some guess on the underlying behavior. This material is presented in Section 6.

2. Theoretical approach for the minimization over the Nehari manifold

Our goal in this section is to present some theoretical elements around ground states and excited states and the Nehari minimization approach. We start by reviewing some well-known facts for the existence and properties of ground states and excited states. We also present the classical variational characterization of ground states as minimizers on the Nehari manifold (see Proposition 2.1). The rest of the section is then devoted to the statement and proof of a characterization of *the first nodal radial excited state* as a minimizer on the Nehari nodal set (see Theorem 2.3). While the approach to obtain Theorem 2.3 borrows elements from the existing literature, the result itself seems to be new.

We consider (2) with solutions belonging to $H^1(\mathbb{R}^d, \mathbb{R})$. A typical example for f is the power-type nonlinearity $f(u) = |u|^{p-1}u$, $1 < p < 2^* - 1$, where 2^* is the critical Sobolev exponent, i.e. $2^* = \frac{2d}{d-2}$ if $d \geqslant 3$, $2^* = \infty$ if $d = 1, 2$. More generally, we assume that $f : \mathbb{R} \to \mathbb{R}$ verifies the following hypotheses (which are not optimal, but sufficient for our purpose).

- **(H1)** (regularity) The function f is continuous and odd.
- **(H2)** (subcriticality) There exists $1 < p < 2^* - 1$ such that for large s, $|f(s)| \lesssim |s|^p$.
- **(H3)** (superlinearity) At 0, $\lim_{s\to 0} \frac{f(s)}{s} = 0$.

(H4) (focusing) There exists $\xi_0 > 0$ such that $F(\xi_0) = \int_0^{\xi_0} f(s)ds > \frac{\xi_0^2}{2}$.

Under **(H1)**-**(H4)**, it is well known (see [6, 7]) that there exist *ground state* solutions, i.e. solutions with minimal action (see (3) for the definition of the action) among all possible solutions to (2). Our definition of ground states as minimal action solutions is very common in the analysis of nonlinear elliptic partial differential equations. The terminology ground state has however several other acceptations in other contexts. E.g. when working with Schrödinger equations modelling Bose-Einstein condensation, one might call ground state a minimizer of the energy on fixed mass constraint.

Uniqueness of the ground state holds if f satisfies in addition to **(H1)**-**(H4)** some complementary requirements, e.g. if f is of power-type, see [20]. When $d \geqslant 2$, it was proved in [6, 8] that there exists an infinite sequence of *excited states*, i.e. solutions to (2) whose action is not minimal (actually, the corresponding sequence of actions tends to infinity). Moreover, under additional assumptions on the nonlinearity (e.g. if $d = 2$ and f is of power-type), then there exists only one radial excited state with a given number of nodes, see [14, 15].

Recall that the action functional $S : H^1(\mathbb{R}^d) \to \mathbb{R}$ is defined in (3). It is a $\mathcal{C}^1$ functional (see e.g. [2]) and u is a solution of (2) if and only if $S'(u) = 0$. We define the *Nehari functional* by

$$I(u) = \langle S'(u), u\rangle = \|\nabla u\|_{L^2}^2 + \|u\|_{L^2}^2 - \int_{\mathbb{R}^d} f(u)udx.$$

The *Nehari manifold* is defined by

$$\mathcal{N} = \{u \in H^1(\mathbb{R}^d) \setminus \{0\} : I(u) = 0\}.$$

Define the *Nehari level* by

$$m_{\mathcal{N}} = \inf\{S(v) : v \in \mathcal{N}\}.$$

In addition to **(H1)**-**(H4)**, we assume the following.

(H5) The function $s \to \frac{f(s)}{s}$ is increasing for $s > 0$.

(H6) (Ambrosetti-Rabinowitz superquadraticity condition) There exists $\theta > 2$ such that $\theta F(s) < sf(s)$ for all $s > 0$.

Then under **(H1)**-**(H6)**, the following holds (see e.g. [25] and the reference cited therein).

Proposition 2.1. *For every sequence $(u_n) \in \mathcal{N}$ such that*

$$\lim_{n\to\infty} S(u_n) = m_{\mathcal{N}},$$

there exist $u_\infty \in \mathcal{N}$ and $(y_n) \subset \mathbb{R}^d$ such that

$$\lim_{n\to\infty} \|u_n(\cdot - y_n) - u_\infty\|_{H^1} = 0.$$

Moreover, u_∞ is a ground state solution of (2).

We now want to construct variational characterizations of excited states which can be used in numerical approaches. Based on Proposition 2.1, it is natural to try to generalize the Nehari manifold approach. Several directions of investigations are possible. The most natural one is probably to define the *Nehari nodal set* as

$$\mathcal{N}_{\text{nod}} = \{u \in H^1(\mathbb{R}^d) : I(u^+) = 0, I(u^-) = 0, u^\pm \neq 0\}.$$

where $u^+ = \max(u, 0)$ and $u^- = \max(-u, 0)$. Define the *Nehari nodal level* by

$$m_{\mathcal{N}_{\rm nod}} = \inf\{S(v) : v \in \mathcal{N}_{\rm nod}\}.$$

Remark 2.2. An approach based on minimization of the energy on mass constraints for the positive and negative part of the function cannot work, as the minimizer that we might obtain would be (formally) a solution of an equation of the form

$$E'(u) + \lambda_+ M'(u_+) + \lambda_- M'(u_-) = 0,$$

with potentially different Lagrange multipliers $\lambda_\pm$. This issue is avoided with the Nehari approach.

We have

$$m_{\mathcal{N}_{\rm nod}} = 2m_{\mathcal{N}}. \tag{4}$$

Indeed, let $u \in \mathcal{N}_{\rm nod}$. Since u^+ and u^- are both in $\mathcal{N}$, we have

$$S(u) = S(u^+) + S(u^-) \geqslant 2m_{\mathcal{N}},$$

and therefore $m_{\mathcal{N}_{\rm nod}} \geqslant 2m_{\mathcal{N}}$. Let u_∞ be a minimizer for $m_{\mathcal{N}}$ and for $(y_n) \subset \mathbb{R}^d$, define

$$u_n = u_\infty(\cdot + y_n) - u_\infty(\cdot - y_n). \tag{5}$$

When $|y_n| \to \infty$, we have

$$S(u_n) \to 2m_{\mathcal{N}},$$

and this proves (4). Unfortunately, $m_{\mathcal{N}_{\rm nod}}$ is not achieved. Indeed, suppose on the contrary that $u_{\rm nod}$ realizes the minimum for $m_{\mathcal{N}_{\rm nod}}$. Since $u^\pm_{\rm nod} \in \mathcal{N}$ and $m_{\mathcal{N}_{\rm nod}} = 2m_{\mathcal{N}}$, both $u^+_{\rm nod}$ and $u^-_{\rm nod}$ realize the minimum for $\mathcal{N}$ and are ground states of (2). In particular, they are both regular, and by the maximum principle, both have to be positive or negative on the whole $\mathbb{R}^d$, which is a contradiction. Therefore $m_{\mathcal{N}_{\rm nod}}$ is not achieved - from (5), we can easily guess that this is due to a loss of compactness in the minimizing sequences. On the other hand, if the power nonlinearity $|u|^{p-1}u$ is replaced by a Choquart/Hartree term (e.g. $(|x|^{-1} * |u|^2)u$ in $\mathbb{R}^3$), then it is possible to obtain nodal critical points by minimizing S on $\mathcal{N}_+ \cap \mathcal{N}_-$, see [18]. To overcome this issue, we decide to work in a radial setting (recall from Strauss' Lemma [23] that the injection $H^1_{\rm rad}(\mathbb{R}^d) \hookrightarrow L^q(\mathbb{R}^d)$, $2 < q < 2^*$ is compact whenever $d \geqslant 2$). Define

$$\mathcal{N}_{\rm nod,rad} = \{u \in H^1_{\rm rad}(\mathbb{R}^d) : I(u^+) = 0, I(u^-) = 0, u^\pm \neq 0\},$$

and

$$m_{\mathcal{N}_{\rm nod,rad}} = \inf\{S(v) : v \in \mathcal{N}_{\rm nod,rad}\}.$$

Then the following result gives the existence of a minimizer for $m_{\mathcal{N}_{\rm nod,rad}}$.

Theorem 2.3. *For every sequence $(u_n) \in \mathcal{N}_{\rm nod,rad}$ such that*

$$\lim_{n\to\infty} S(u_n) = m_{\mathcal{N}_{\rm nod,rad}}$$

there exists $u_\infty \in \mathcal{N}_{\rm nod,rad}$ such that

$$\lim_{n\to\infty} \|u_n - u_\infty\|_{H^1} = 0.$$

Moreover, u_∞ is a nodal solution of (2) with exactly two nodal domains. We say that u_∞ is a least nodal excited state.

Remark 2.4. Minimizing on $\mathcal{N}_{\mathrm{nod,rad}}$ is intrinsically more difficult that minimizing on $\mathcal{N}$. Indeed, $\mathcal{N}_{\mathrm{nod,rad}}$ is *not* a manifold, as the functionals

$$u \in H^1(\mathbb{R}^d) \to \|\nabla u^{\pm}\|_{L^2}^2$$

are *not* $\mathcal{C}^1$ (see the discussion after Theorem 18 in [25]).

The rest of this section is devoted to the proof of Theorem 2.3. We start with some preliminary lemmas.

Lemma 2.5. *The constant* 0 *is a local minimum for* S. *Let* $u \in H^1(\mathbb{R}^d) \setminus \{0\}$. *There exists a unique* $s_u \in (0,\infty)$ *such that* $I(s_u u) = 0$. *Moreover,* $S(s_u u) = \max_{s\in(0,\infty)} S(su) > 0$. *If* $I(u) < 0$, *then* $s_u < 1$, *whereas if* $I(u) > 0$, *then* $s_u > 1$ *and* $S(u) > 0$.

Proof. Let $u \in H^1(\mathbb{R}^d) \setminus \{0\}$ and define $h : (0,\infty) \to \mathbb{R}$ by

$$h(s) := S(su) = \frac{s^2}{2}\|u\|_{H^1}^2 - \int_{\mathbb{R}} F(su)dx.$$

Since F is differentiable, so is h and we have

$$h'(s) = s\|u\|_{H^1}^2 - \int_{\mathbb{R}} f(su)udx.$$

Remark that $sh'(s) = I(su)$. Due to **(H5)**, the derivative h' can vanish only once in $(0,\infty)$. Indeed, assume by contradiction that there exist $0 < s_1 < s_2$ such that $h'(s_1) = h'(s_2) = 0$. Then we have

$$\int_{\mathbb{R}} \frac{f(s_1u)}{s_1u}u^2dx = \int_{\mathbb{R}} \frac{f(s_2u)}{s_2u}u^2dx.$$

Since by **(H5)** $s \to \frac{f(s)}{s}$ is increasing, we have a contradiction. Since $f(s) = o(s)$ for $s \to 0$, we have $S(su) > 0$ if s is small enough. On the other hand, **(H6)** implies that

$$\partial_s \frac{F(s)}{s^2} = \frac{f(s)s - 2F(s)}{s^3} > \frac{(\theta-2)}{s}\frac{F(s)}{s^2},$$

i.e. F is superquadratic and therefore for s large we must have $S(su) < 0$. Hence h' vanishes exactly once at s_u, $h'(s) > 0$ for $s < s_u$ and $h'(s) < 0$ for $s > s_u$. Moreover, $h(s_u) = \max_{s\in(0,\infty)} h(s)$. Since $S(su) = h(s)$ and $I(su) = sh'(s)$, this concludes the proof. □

Define $\mathcal{N}_{\mathrm{rad}} := \mathcal{N} \cap H^1_{\mathrm{rad}}(\mathbb{R}^d)$. We have the following compactness result.

Lemma 2.6. *Let* $d \geqslant 2$. *Let* $(u_n) \subset \mathcal{N}_{\mathrm{rad}}$ *and assume that* $S(u_n)$ *is bounded. Then* (u_n) *is bounded in* $H^1(\mathbb{R}^d)$ *and there exists* $u_\infty \in H^1_{\mathrm{rad}}(\mathbb{R}) \setminus \{0\}$ *such that (up to extraction of a subsequence) we have*

$$u_n \rightharpoonup u_\infty \text{ weakly in } H^1_{\mathrm{rad}}(\mathbb{R}).$$

Moreover, there exists $s_\infty > 0$ *such that* $s_\infty u_\infty \in \mathcal{N}_{\mathrm{rad}}$ *and* $S(s_\infty u_\infty) \leqslant \liminf_{n\to\infty} S(u_n)$.

Proof. Take a sequence $(u_n) \in \mathcal{N}_{\mathrm{rad}}$ and assume that $S(u_n)$ is bounded. Arguing by contradiction, we assume that $\nu_n := \|u_n\|_{H^1} \to \infty$. Define a sequence $(v_n) \subset H^1_{\mathrm{rad}}(\mathbb{R}^d)$ by

$$v_n := \frac{u_n}{\nu_n}.$$

Then (v_n) is bounded in $H^1_{\rm rad}(\mathbb{R}^d)$ and there exists $v_\infty \in H^1_{\rm rad}(\mathbb{R}^d)$ such that $v_n \rightharpoonup v_\infty$ weakly in $H^1_{\rm rad}(\mathbb{R}^d)$. We claim that $v_\infty \neq 0$. Arguing again by contradiction, assume that $v_\infty = 0$. By Lemma 2.5, for any $s > 0$, we have

$$S(u_n) = S(\nu_n v_n) \geqslant S(sv_n) = \frac{s^2}{2} - \int_{\mathbb{R}} F(sv_n)dx.$$

Since $d \geqslant 2$, the injection $H^1_{\rm rad}(\mathbb{R}^d) \hookrightarrow L^q(\mathbb{R}^d)$ is compact for any $2 < q < 2^*$. Combined with **(H2)**, this implies weak continuity of $u \to \int_{\mathbb{R}^d} F(u)dx$. Since we assumed $v_\infty = 0$, for n large we have

$$S(u_n) \geqslant \frac{s^2}{4},$$

which is a contradiction since $S(u_n)$ is bounded and s can be chosen a large as desired. Hence $v_\infty \neq 0$. Moreover, since $I(u_n) = 0$, we have

$$0 \leqslant \frac{S(u_n)}{\nu_n^2} = \frac{1}{2} - \frac{1}{\nu_n^2}\int_{\mathbb{R}} F(\nu_n v_n)dx. \tag{6}$$

From **(H6)**, we have $F(s) \geqslant s^\theta$, thus

$$\lim_{s\to\infty} \frac{F(s)}{s^2} = \infty.$$

Recall that upon extraction of subsequences, $v_n \rightharpoonup v_\infty \neq 0$ weakly in $H^1_{\rm rad}(\mathbb{R}^d)$ and $v_n(x) \to v_\infty(x)$ a.e. By Fatou's Lemma, this implies

$$\frac{1}{\nu_n^2}\int_{\mathbb{R}} F(\nu_n v_n)dx = \int_{\mathbb{R}} \frac{F(\nu_n v_n)}{(\nu_n v_n)^2} v_n^2 dx \to \infty \text{ as } n \to \infty.$$

This leads to a contradiction in (6). Therefore, $(\nu_n) = (\|u_n\|_{H^1})$ has to remain bounded. As a consequence, there exists $u_\infty \in H^1_{\rm rad}(\mathbb{R}^d)$ such that $u_n \rightharpoonup u_\infty$. We can prove that $u_\infty \neq 0$ in the same way as we did for v_∞. Moreover, there exists s_∞ such that $s_\infty u_\infty \in \mathcal{N}_{\rm rad}$ and we have

$$S(s_\infty u_\infty) \leqslant \liminf_{n\to\infty} S(s_\infty u_n) \leqslant \liminf_{n\to\infty} S(u_n).$$

This concludes the proof. □

Proof of Theorem 2.3. Let (u_n) be a minimizing sequence for $m_{\mathcal{N}_{\rm nod,rad}}$, i.e. $(u_n) \subset \mathcal{N}_{\rm nod,rad}$ and $S(u_n) \to m_{\mathcal{N}_{\rm nod,rad}}$ as $n \to \infty$. Since $(u_n^\pm) \subset \mathcal{N}$, by Lemma 2.6 the sequence $(u_n^\pm)$ is bounded in $H^1_{\rm rad}(\mathbb{R}^d)$ and there exists $\tilde{u}_\infty^\pm \in H^1_{\rm rad}(\mathbb{R}^d) \setminus \{0\}$ such that $u_n^\pm \rightharpoonup \tilde{u}_\infty^\pm$ weakly in $H^1_{\rm rad}(\mathbb{R}^d)$ and a.e. In particular, pointwise convergence implies $\tilde{u}_\infty^+ \tilde{u}_\infty^- = 0$ a.e. Let $s^\pm$ be such that $I(s^\pm \tilde{u}_\infty^\pm) = 0$ and define

$$u_\infty = s^+ \tilde{u}_\infty^+ - s^- \tilde{u}_\infty^-.$$

By construction $u_\infty \in \mathcal{N}_{\rm nod,rad}$. Moreover,

$$S(u_\infty) = S(s^+\tilde{u}_\infty^+) + S(s^-\tilde{u}_\infty^-) \leqslant \liminf_{n\to\infty}(S(u_n^+) + S(u_n^-)) = \lim_{n\to\infty} S(u_n) = m_{\mathcal{N}_{\rm nod,rad}}.$$

This proves that u_∞ is a minimizer for $m_{\mathcal{N}_{\rm nod,rad}}$.

Let us show that in fact $s^\pm = 1$ and the sequence (u_n) converges strongly in $H^1_{\rm rad}(\mathbb{R}^d)$ toward u_∞. By **(H2)** and Strauss' Lemma, the functional $u \mapsto \int_{\mathbb{R}^d} f(u)udx$ is weakly continuous on $H^1_{\rm rad}(\mathbb{R}^d)$. This implies

$$I(\tilde{u}_\infty^\pm) \leqslant \liminf_{n\to\infty} I(u_n^\pm) = 0.$$

Hence by Lemma 2.5 we have $s^{\pm} \leqslant 1$. Moreover

$$m_{\mathcal{N}_{\mathrm{nod,rad}}} \leqslant S(u_\infty) \leqslant \liminf_{n\to\infty} (S(u_n^+) + S(u_n^-)) = m_{\mathcal{N}_{\mathrm{nod,rad}}}$$

and weak continuity of the nonlinear part of S imply

$$\|u_\infty\|_{H^1}^2 = \liminf_{n\to\infty} \left(\|u_n^+\|_{H^1}^2 + \|u_n^-\|_{H^1}^2\right). \tag{7}$$

Moreover

$$\begin{aligned}\liminf_{n\to\infty} \left(\|u_n^+\|_{H^1}^2 + \|u_n^-\|_{H^1}^2\right) &\geqslant \|\tilde{u}_\infty^+ - \tilde{u}_\infty^-\|_{H^1}^2 = \frac{1}{(s^+)^2}\|s^+\tilde{u}_\infty^+\|_{H^1}^2 + \frac{1}{(s^-)^2}\|s^-\tilde{u}_\infty^-\|_{H^1}^2 \\ &\geqslant \frac{1}{\max(s^-,s^+)^2}(\|s^+\tilde{u}_\infty^+\|_{H^1}^2 + \|s^-\tilde{u}_\infty^-\|_{H^1}^2) = \frac{1}{\max(s^-,s^+)^2}\|u_\infty\|_{H^1}^2 \\ &= \frac{1}{\max(s^-,s^+)^2}\liminf_{n\to\infty} \left(\|u_n^+\|_{H^1}^2 + \|u_n^-\|_{H^1}^2\right).\end{aligned}$$

where the first inequality is from weak convergence and the last equality follows from (7). Since we already know that $s^{\pm} \leqslant 1$, this implies that $s^{\pm} = 1$ and strong convergence of (u_n) towards u_∞ in $H^1(\mathbb{R}^d)$.

We now show that u_∞ is a critical point of S. Recall that $\mathcal{N}_{\mathrm{nod,rad}}$ is not a manifold and we cannot use a Lagrange multiplier argument for the minimizers of $m_{\mathcal{N}_{\mathrm{nod,rad}}}$. Instead, we shall use the quantitative deformation lemma of Willem [26, Lemma 2.3], which we recall in Appendix (see Lemma A.1). Arguing by contradiction, we assume that $S'(u_\infty) \neq 0$. Then there exist $\delta, \mu > 0$ such that

$$\|v - u_\infty\|_{H^1} \leqslant 3\delta \implies \|S'(u_\infty)\|_{H^1} \geqslant \mu.$$

Define $D = \left[\frac{1}{2}, \frac{3}{2}\right] \times \left[\frac{1}{2}, \frac{3}{2}\right]$ and $g(s,t) = su_\infty^+ - tu_\infty^-$. Let $s, t > 0$ be such that either $s \neq 1$ or $t \neq 1$. Then from **(H5)** we infer that

$$S(su_\infty^+ - tu_\infty^-) = S(su_\infty^+) + S(tu_\infty^-) < S(u_\infty^+) + S(u_\infty^-) = m_{\mathcal{N}_{\mathrm{nod,rad}}}.$$

Consequently, $S(g(s,t)) = m_{\mathcal{N}_{\mathrm{nod,rad}}}$ if and only if $s = t = 1$ and otherwise $S(g(s,t)) < m_{\mathcal{N}_{\mathrm{nod,rad}}}$. Hence

$$\beta := \max_{\partial D} S \circ g < m_{\mathcal{N}_{\mathrm{nod,rad}}}.$$

Let $\varepsilon := \min\left(\frac{m_{\mathcal{N}_{\mathrm{nod,rad}}} - \beta}{4}, \frac{\mu\delta}{8}\right)$. The deformation lemma A.1 gives us a deformation η verifying

(a) $\eta(1,v) = v$ if $v \notin S^{-1}([m_{\mathcal{N}_{\mathrm{nod,rad}}} - 2\varepsilon, m_{\mathcal{N}_{\mathrm{nod,rad}}} + \varepsilon])$,
(b) $S(\eta(1,v)) \leqslant m_{\mathcal{N}_{\mathrm{nod,rad}}} - \varepsilon$ for every $v \in H^1_{\mathrm{rad}}(\mathbb{R}^d)$ such that $\|v - u_\infty\|_{H^1} \leqslant \delta$ and $S(v) \leqslant m_{\mathcal{N}_{\mathrm{nod,rad}}} + \varepsilon$,
(c) $S(\eta(1,v)) \leqslant S(v)$ for all $v \in H^1_{\mathrm{rad}}(\mathbb{R}^d)$.

In particular, we have

$$\max_{(s,t)\in D} S(\eta(1, g(s,t))) < m_{\mathcal{N}_{\mathrm{nod,rad}}}. \tag{8}$$

To obtain a contradiction we prove that $\eta(1, g(D)) \cap \mathcal{N}_{\mathrm{nod,rad}} \neq \emptyset$. Define $h(s,t) := \eta(g(1, g(s,st)))$ and

$$\psi_0(s,t) := \left(I(su_\infty^+), I(tu_\infty^-)\right), \quad \psi_1(s,t) := \left(I(h^+(s,t)), I(h^-(s,t))\right),$$

As $I(su_\infty^{\pm}) > 0$ (resp. < 0) if $0 < s < 1$ (resp. $s > 1$), the degree of ψ_0 (see e.g. [1] for the definition and basic properties of the degree) is $\mathrm{Deg}(\psi_0, D, 0) = 1$. From (a) and (8), we have $g = h$ on ∂D. Therefore, $\psi_0 = \psi_1$ on ∂D, which implies

$\mathrm{Deg}(\psi_1, D, 0) = 1 = \mathrm{Deg}(\psi_0, D, 0) = 1$. Therefore, there exists $(s,t) \in D$ such that $\psi_1(s,t) = 0$. That means $h(s,t) \in \mathcal{N}_{\mathrm{nod,rad}}$, a contradiction with (8) and the definition of $m_{\mathcal{N}_{\mathrm{nod,rad}}}$. Therefore u_∞ is a critical point of S.

It remains to prove that u_∞ has exactly two nodal domains. Observe first that u_∞ is also a minimizer for

$$m_{alt} = \inf \left\{ \int_{\mathbb{R}^d} -F(u) + \frac{1}{2} f(u)u dx : I(u^+) \leqslant 0,\ I(u^-) \leqslant 0,\ u^\pm \neq 0 \right\}.$$

By **(H6)**, $2F(s) - f(s)s < 0$ for any s. As a consequence, the minimizers of m_{alt} verify $I(u^+) = I(u^-) = 0$. Indeed, arguing by contradiction and assuming e.g. $I(u^+) < 0$, one could replace u^+ by tu^+ with $0 < t < 1$ such that $I(tu^+) = 0$, which would give a minimizer of m_{alt} for a lower value and provides the contradiction. Assume now that u_∞ has more than one nodal region, i.e that there exists $s_1 < s_2 < s_3$ such that $u_\infty > 0$ on $(0, s_1)$, $u_\infty < 0$ on (s_1, s_2) and $u_\infty > 0$ on (s_2, s_3). Let u_1 be such that $u_1 = u_\infty$ on $(0, s_1)$ and $u_1 = 0$ elsewhere. Define similarly u_2 for (s_1, s_2) and $u_3^\pm = u_\infty^\pm$, on (s_3, ∞). Since $I(u^+) = 0$ we either have $I(u_1) \leqslant 0$ or $I(u_3^+) \leqslant 0$. Without loss of generality, assume that $I(u_1) \leqslant 0$. We may then construct $\tilde{u}_\infty$ such that $\tilde{u}_\infty = u_1$ on $(0, s_1)$, $\tilde{u}_\infty = u_2$ on (s_1, s_2) and $\tilde{u}_\infty = 0$ on (s_3, ∞). As it is not containing the $u_3^\pm$ parts, $\tilde{u}_\infty$ would be a minimizer for m_{alt} for a lower value than u_∞, which provides a contradiction and finishes the proof. □

3. The shooting method

We describe in this section the shooting method, its theoretical background and its practical implementation. Radial solutions of (2) can be obtained as solutions of the ordinary differential equation

$$-u''(r) - \frac{d-1}{r} u'(r) + \omega u(r) - f(u(r)) = 0. \tag{9}$$

They should satisfy the boundary conditions

$$u'(0) = 0, \quad \lim_{r \to \infty} u(r) = 0.$$

It was established in [15] that, under convexity assumptions on f (which hold for example in dimension $d = 2$ when f is of power-type), that for any $k \in \mathbb{N}$, the equation (9) admits exactly one solution having exactly k nodes. More precisely, it was proved in [15] that there exists an increasing sequence $(\alpha_k) \subset (0, \infty)$ such that for any $k \in \mathbb{N}$ and for any $\alpha \in (\alpha_{k-1}, \alpha_k)$ (with the understanding that $\alpha_{-1} = 0$), the solution of the Cauchy Problem

$$-u''(r) - \frac{d-1}{r} u'(r) + \omega u(r) - f(u(r)) = 0, \quad u(0) = \alpha, \quad u'(0) = 0, \tag{10}$$

denoted by $u(\cdot; \alpha)$, has exactly k nodes on $[0, \infty)$. Moreover, when (and only when) $\alpha = \alpha_k$, the solution $u(\cdot; \alpha_k)$ of (10) verifies

$$\lim_{r \to \infty} u(r; \alpha_k) = 0.$$

In other words, finding the k-th radial state amounts to finding the corresponding α_k. We expect that $k \sim \alpha_k^2$ (see Figure 7). Observe that when $\alpha \in (\alpha_k, \alpha_{k+1})$, then the solution of the differential equation such that $u(0) = \alpha$ has exactly k nodes (but does not converge to 0 at infinity).

The so-called shooting method then consists in a simple application of the bisection principle to the search of α_k. The idea is the following. Start with an

interval $[\alpha_*, \alpha^*]$ such that $u(\cdot;\alpha_*)$ and $u(\cdot;\alpha^*)$ have respectively $k-1$ and k nodes on $(0,\infty)$. Define the middle of $[\alpha_*, \alpha^*]$ by $c_* = (\alpha_* + \alpha^*)/2$. If the solution $u(\cdot;c_*)$ with initial data c_* has $k-1$ nodes on $(0,\infty)$, then reproduce the procedure on $[c_*, \alpha^*]$, otherwise iterate the procedure on $[\alpha_*, c_*]$. The interval size is divided by two at each step and its bounds converge towards α_k.

To compute the solution of (9), we rewrite it as a first order system

$$U'(r) = AU + F(r, U(r)), \quad U(0) = \begin{pmatrix} \alpha \\ 0 \end{pmatrix} \tag{11}$$

where

$$U(r) = \begin{pmatrix} u(r) \\ u'(r) \end{pmatrix}, \quad A = \begin{pmatrix} 0 & 1 \\ \omega & 0 \end{pmatrix}, \quad F(r, U(r)) = \begin{pmatrix} 0 \\ \frac{d-1}{r} u'(r) + f(u(r)) \end{pmatrix}.$$

The solution of the initial value problem (11) is then computed using the classical Runge-Kutta 4th order method. The only difficulty concerns the value to affect to F at $r = 0$. The singularity can in fact be raised when u is sufficiently regular and the initial condition contains $u'(0) = 0$. Indeed, assuming that $u' \in \mathcal{C}^2$ and writing the Taylor expansion at 0, we have

$$u'(r) = u'(0) + u''(0)r + u'''(\theta)\frac{r^2}{2} = u''(0)r + u'''(\theta)\frac{r^2}{2}, \quad \theta \in (0, r).$$

Assuming that u verifies (9), we have

$$-u''(r) - (d-1)u''(0) + u'''(\theta)\frac{(d-1)r}{2} + \omega u(r) - f(u(r)) = 0.$$

Letting r tend to 0, we obtain

$$-du''(0) + \omega u(0) - f(u(0)) = 0.$$

Therefore, we choose to set

$$F\begin{pmatrix} u(0) \\ 0 \end{pmatrix} = \begin{pmatrix} 0 \\ (\omega u(0) - f(u(0)))/d \end{pmatrix}.$$

Algorithm 1 The Shooting Method Algorithm.

Require: F, ε, `nb_expected_nodes`, $b > 0$
  $a \leftarrow 0$
  while $|a - b| < \varepsilon$ **do**
    $c \leftarrow (a + b)/2$
    `Solve` $Y' = F(t, Y)$, $Y(0) = c$ with RK4
    `nb_nodes` $\leftarrow$ number of nodes of Y
    if `nb_nodes` $>$ `nb_expected_nodes` **then**
      $b \leftarrow c$
    else
      $a \leftarrow c$
    end if
  end while

The algorithm is given in Algorithm 1. Note that in Algorithm 1, it is understood that b has been chosen large enough so that the initial data of the excited state with the required number of nodes lies in $[0, b]$. In pratice, such a b can be obtained

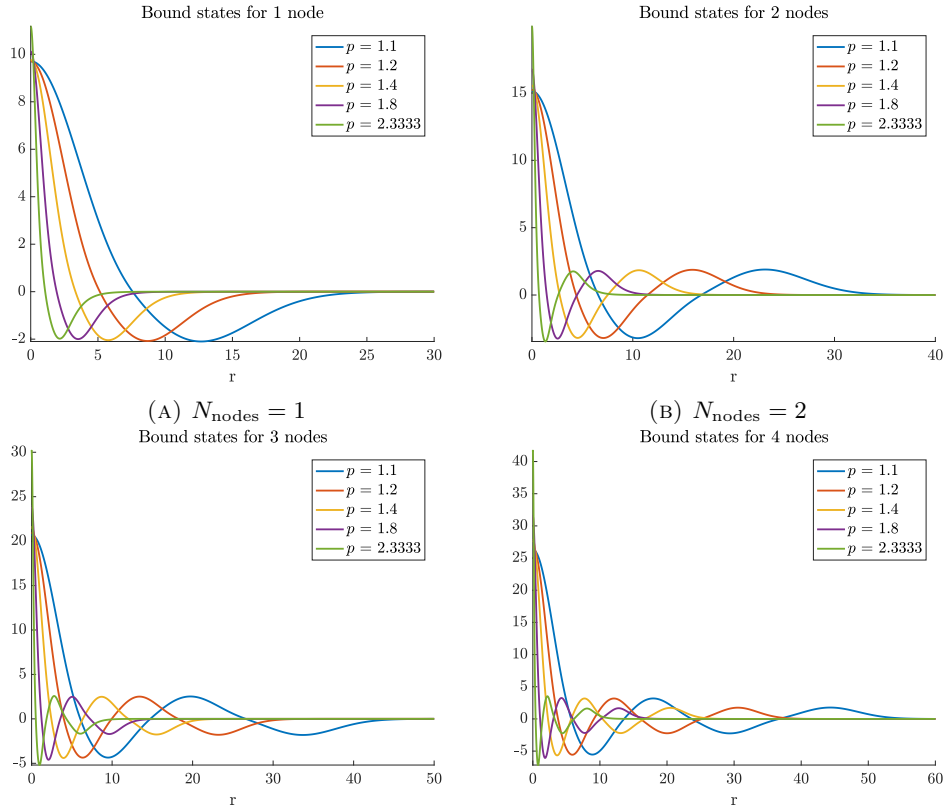

(A) $N_{\text{nodes}} = 1$ (B) $N_{\text{nodes}} = 2$

(C) $N_{\text{nodes}} = 3$ (D) $N_{\text{nodes}} = 4$

FIGURE 1. Bound states in dimension $d = 3$

by inspection, taking larger and larger values until the solution of (10) with initial data $\alpha = b$ has a sufficiently large number of nodes.

Examples of solutions computed with the Shooting method are presented in Figure 1.

4. The Nehari method

In this section, we assume that $f(u) = |u|^{p-1}u$ with $p \in (1, 1 + 4/(d-2)_+)$. and we consider the problem

$$-\Delta u + u - |u|^{p-1}u = 0$$

on Ω where $\Omega \subset \mathbb{R}^d$ is a domain or $\mathbb{R}^d$ itself. We recall that the action functional S is given by

$$S(u) = \frac{1}{2}\|\nabla u\|^2_{L^2(\Omega)} + \frac{1}{2}\|u\|^2_{L^2(\Omega)} - \frac{1}{p+1}\|u\|^{p+1}_{L^{p+1}(\Omega)},$$

and the Nehari functional

$$I(u) = \|\nabla u\|^2_{L^2(\Omega)} + \|u\|^2_{L^2(\Omega)} - \|u\|^{p+1}_{L^{p+1}(\Omega)}.$$

The Nehari manifold on Ω is then given by

$$\mathcal{N} = \left\{u \in H^1_0(\Omega) : I(u) = 0\right\}.$$

To compute numerically nodal solutions when $\Omega = \mathbb{R}^d$, an approach based on Theorem 2.3 would provide only the least nodal excited state. As we would also like to compute higher order excited states, we will adopt a slightly different setting and we base our the approach on the theoretical result obtained by Bartsch and Willem [5], which we describe now. Let $\Omega(\rho, \sigma) \subset \mathbb{R}^d$ be the annulus of $\mathbb{R}^d$ of radii ρ and σ:

$$\Omega(\rho, \sigma) = \{x \in \mathbb{R}^d : \rho \leqslant |x| < \sigma\}.$$

To obtain radial nodal excited states, we first work on each $\Omega(\rho, \sigma)$.

Lemma 4.1. *For all $0 \leqslant \rho < \sigma \leqslant \infty$ there exists a positive minimizer $w_{\rho,\sigma} \in H_0^1(\Omega(\rho, \sigma))$ of the action on the Nehari manifold on $\Omega(\rho, \sigma)$, i.e.*

$$S(w_{\rho,\sigma}) = m_{\rho,\sigma} := \min\{S(u) : u \in \mathcal{N}\},$$

where it is understood that we have replaced Ω by $\Omega(\rho, \sigma)$ in the definitions of S, I and $\mathcal{N}$.

Nodal excited states are obtained by pasting together different w_{ρ_j,σ_j} and optimizing over (ρ_j, σ_j). More precisely, we have the following result from [5].

Proposition 4.2. *For every integer $N_{nodes} \geqslant 0$ there exists a radial solution $u_{N_{nodes}}$ of (4) having exactly N_{nodes} nodes, i.e. there exist $0 = \rho_0 < \rho_1 < \cdots < \rho_{N_{nodes}} < \rho_{N_{nodes}+1} = \infty$ such that*

$$u_k^{-1}(0) = \{x \in \mathbb{R}^d : |x| = \rho_j, \text{ for some } j = 1, \dots, N_{nodes}\}.$$

The set $(\rho_j)_{j=0,\dots,N_{nodes}+1}$ is the minimizer of

$$\min\left\{\sum_{j=0}^{N_{nodes}} m_{\rho_j,\rho_{j+1}} : 0 = \rho_0 < \rho_1 < \cdots < \rho_{N_{nodes}} < \rho_{N_{nodes}+1} = \infty\right\}.$$

The function $u_{N_{nodes}}$ is constructed with the $w_{\rho_j,\rho_{j+1}}$ corresponding to $m_{\rho_j,\rho_{j+1}}$:

$$u_{N_{nodes}}(x) = (-1)^j w_{\rho_j,\rho_{j+1}}(x), \text{ if } \rho_j \leqslant |x| < \rho_{j+1}.$$

Of course, if one wishes to compute numerically such a sequence, we must restrict ourselves to a bounded interval. That is, instead of considering the problem on the whole line $\mathbb{R}$, we restrict ourselves to the interval $[0, R]$ for a given $R > 0$ sufficiently large. We consider the space

$$\mathcal{H}^1_{\mathrm{rad},R} := \left\{u : [0, R] \mapsto \mathbb{R} : \int_0^R (|u'(r)|^2 + |u(r)|^2) r^{d-1} dr < +\infty,\ u(R) = 0\right\},$$

on which we define the functionals S and I by the same formula, but restricted to the interval $[0, R]$. Similarly, we define the nodal Nehari space

$$\mathcal{N}_{N_{\mathrm{nodes}},R} := \left\{u \in \mathcal{H}^1_{\mathrm{rad},R} : u^{-1}(0) = \{\rho_1, \rho_2, \dots, \rho_{N_{\mathrm{nodes}}}\},\ I(u_{|[\rho_k,\rho_{k+1}]}) = 0,\ 0 \leqslant k \leqslant N_{\mathrm{nodes}}\right\},$$

where $0 = \rho_0 < \rho_1 < \ldots < \rho_{N_{\mathrm{nodes}}+1} = R$ are depending on u. Let

$$\mathcal{H}_{N_{\mathrm{nodes}},R} := \left\{u \in \mathcal{H}^1_{\mathrm{rad},R} \middle|\ u^{-1}(0) = \{\rho_1, \rho_2, \dots, \rho_{N_{\mathrm{nodes}}}\}\right\}.$$

Then, we define the projection $\Pi_{\mathcal{N}_{N_{\mathrm{nodes}},R}} : \mathcal{H}_{N_{\mathrm{nodes}},R} \mapsto \mathcal{N}_{N_{\mathrm{nodes}},R}$ by

$$\Pi_{\mathcal{N}_{N_{\mathrm{nodes}}}} u := \sum_{k=0}^{N_{\mathrm{nodes}}} u_{|[\rho_k,\rho_{k+1}]} \left(\frac{\|\nabla u_{|[\rho_k,\rho_{k+1}]}\|^2_{L^2} + \|u_{|[\rho_k,\rho_{k+1}]}\|^2_{L^2}}{\|u_{|[\rho_k,\rho_{k+1}]}\|^{p+1}_{L^{p+1}}}\right)^{1/(p-1)}.$$

A natural method to compute the solution of

$$\min_{u\in\mathcal{N}_{N_{\rm nodes},R}} S(u),$$

is to use the so-called projected gradient descent given by

$$\left\{\begin{array}{l} u^{(0)}\in\mathcal{N}_{N_{\rm nodes},R},\\ u^{(n+1)}=\Pi_{\mathcal{N}_{N_{\rm nodes},R}}\left(u^{(n)}+\tau S'(u^{(n)})\right), \quad \forall n\geqslant 0,\end{array}\right.$$

where $\tau\in\mathbb{R}^+$ is the time-step, which also writes as

$$\left\{\begin{array}{l} u^{(0)}\in\mathcal{N}_{N_{\rm nodes},R},\\ u^{(n+1)}=\Pi_{\mathcal{N}_{N_{\rm nodes},R}}\left(u^{(n)}-\tau(\Delta_{{\rm rad},R}u^{(n)}-u^{(n)}+|u^{(n)}|^{p-1}u^{(n)})\right), \quad \forall n\geqslant 0.\end{array}\right.$$

By setting $\pi_N([0,R]):=\{r_k:=(k-1)h,\ 1\leqslant k\leqslant N+1\}$ with $h=R/N$, we can consider a discretization of $\Delta_{{\rm rad},R}$ by finite differences acting on $\mathbb{R}^N$. That is, for any $u\in\mathcal{H}^1_{{\rm rad},R}$ we use the second order approximations, for any $2\leqslant k\leqslant N-1$,

$$u''(r_k)\approx\frac{u(r_{k+1})-2u(r_k)+u(r_{k-1})}{h^2} \quad\text{and}\quad u'(r_k)\approx\frac{u(r_{k+1})-u(r_{k-1})}{2h}, \quad (12)$$

to deduce the following approximation

$$\Delta_{{\rm rad},R}u(r_k)\approx\frac{u(r_{k+1})-2u(r_k)+u(r_{k-1})}{h^2}+\frac{d-1}{r_k}\frac{u(r_{k+1})-u(r_{k-1})}{2h}.$$

Furthermore, the boundary conditions yield

$$\begin{aligned}\Delta_{{\rm rad},R}u(r_1)&\approx\frac{2(u(r_2)-u(r_1))}{h^2}\\ \text{and}\quad \Delta_{{\rm rad},R}u(r_N)&\approx\frac{-2u(r_N)+u(r_{N-1})}{h^2}-\frac{d-1}{r_N}\frac{u(r_{N-1})}{2h}.\end{aligned}$$

In the end, we obtain the matrix

$$[\Delta_{{\rm rad},R}]_{i,j}:=\left\{\begin{array}{ll} 2/h^2, & \text{for } (i,j)=(1,2),\\ -2/h^2, & \text{for } 1\leqslant i\leqslant N \text{ and } j=i,\\ 1/h^2-(d-1)/2hr_i, & \text{for } 2\leqslant i\leqslant N \text{ and } j=i-1,\\ 1/h^2+(d-1)/2hr_i, & \text{for } 2\leqslant i\leqslant N-1 \text{ and } j=i+1,\\ 0, & \text{else.}\end{array}\right.$$

By denoting $\boldsymbol{u}=(u(r_j))_{1\leqslant j\leqslant N}\in\mathbb{R}^N$ as the discretization of u on $\pi_N([0,R])$, we deduce that

$$\Delta_{{\rm rad},R}u(r_i)\approx([\Delta_{{\rm rad},R}]\boldsymbol{u})_i, \quad \forall i\in\{1,\dots,N\}.$$

We also need to discretize the positions of the nodes $\{\rho_1,\dots,\rho_{N_{\rm nodes}}\}$ and the projection on $\mathcal{N}_{N_{\rm nodes},R}$. For any $u\in\mathcal{H}^1_{{\rm rad},R}$, each node of u is located in an interval $[r_j,r_{j+1}]$, for a certain $1\leqslant j\leqslant N$, where $u(r_{j+1})u(r_j)<0$. By a linear approximation of u on each interval $[r_j,r_{j+1}]$, with $1\leqslant j\leqslant N$, an approximation of a node ρ belonging in $[r_j,r_{j+1}]$ will be given by

$$\rho\approx\varrho=\frac{r_ju(r_{j+1})-r_{j+1}u(r_j)}{u(r_{j+1})-u(r_j)}. \quad (13)$$

Concerning the projection on $\mathcal{N}_{N_{\rm nodes},R}$, we need approximations of integrals and we choose to rely on a trapezoidal rule. This yields, for any $v\in\mathcal{C}([0,R])$,

$$\int_a^b v(r)r^{d-1}dr\approx\frac{v(b)b^{d-1}+v(a)a^{d-1}}{2}(b-a).$$

We denote $(\rho_k)_{0\leqslant k\leqslant N_{\rm nodes}+1}$ the nodes of u with $\rho_0 = 0$ and $\rho_{N_{\rm nodes}+1} = R$. For any $u \in \mathcal{H}^1_{{\rm rad},R}$ and $0 \leqslant k \leqslant N_{\rm nodes}$, we deduce the approximation (using the trapezoidal rule)

$$\begin{aligned}\|u_{|[\rho_k,\rho_{k+1}]}\|^p_{L^p} &= \int_{\rho_k}^{\rho_{k+1}} |u(r)|^p r^{d-1} dr \\ &\approx h \sum_{j=m(\varrho_k)}^{\ell(\varrho_{k+1})} |u(r_j)|^p r_j^{d-1} + \frac{(r_{m(\varrho_k)} - \varrho_k) - h}{2} |u(r_{m(\varrho_k)})|^p r_{m(\varrho_k)}^{d-1} \\ &\quad + \frac{(\varrho_{k+1} - r_{\ell(\varrho_{k+1})}) - h}{2} |u(r_{\ell(\varrho_{k+1})})|^p r_{\ell(\varrho_{k+1})}^{d-1} := \mathfrak{L}^p_k(\boldsymbol{u}), \quad (14)\end{aligned}$$

where $m(\rho) = \min\{j \in \{1,\dots,N\} :\ r_j \geqslant \rho\}$, $\ell(\rho) = \max\{j \in \{1,\dots,N\} :\ r_j \leqslant \rho\}$ and ϱ_k is the approximation of ρ_k obtained by (13). Furthermore, we have, by using (12), for any $u \in \mathcal{H}^1_{{\rm rad},R}$ and $1 \leqslant k \leqslant N_{\rm nodes} - 1$,

$$\begin{aligned}\|\nabla u_{|[\rho_k,\rho_{k+1}]}\|^2_{L^2} &\approx h \sum_{j=m(\varrho_k)}^{\ell(\varrho_{k+1})} \left|\frac{u(r_{j+1}) - u(r_{j-1})}{2h}\right|^2 r_j^{d-1} \\ &\quad + \frac{(r_{m(\varrho_k)} - \varrho_k) - h}{2} \left|\frac{u(r_{m(\varrho_k)+1}) - u(r_{m(\varrho_k)-1})}{2h}\right|^2 r_{m(\varrho_k)}^{d-1} \\ &\quad + \frac{r_{m(\varrho_k)} - \varrho_k}{2} \left|\frac{u(r_{m(\varrho_k)}) - u(r_{m(\varrho_k)-1})}{h}\right|^2 \varrho_k^{d-1} \\ &\quad + \frac{(\varrho_{k+1} - r_{\ell(\varrho_{k+1})}) - h}{2} \left|\frac{u(r_{\ell(\varrho_{k+1})+1}) - u(r_{\ell(\varrho_{k+1})-1})}{2h}\right|^2 r_{\ell(\varrho_{k+1})}^{d-1} \\ &\quad + \frac{\varrho_{k+1} - r_{\ell(\varrho_{k+1})}}{2} \left|\frac{u(r_{\ell(\varrho_{k+1})+1}) - u(r_{\ell(\varrho_{k+1})})}{h}\right|^2 \varrho_{k+1}^{d-1} \\ &:= \mathfrak{N}_k(\boldsymbol{u}), \quad (15)\end{aligned}$$

where we used the following finite differences approximation

$$u'(\rho) \approx \frac{u(r_j) - u(r_{j-1})}{r_j - r_{j-1}},$$

with $j \in \{1,\dots,N\}$ such that ρ is a nod belonging in (r_{j-1}, r_j). We notice that, in the case $k = N_{\rm nodes}$, the previous expression is replaced with

$$\begin{aligned}\|\nabla u_{|[\rho_{N_{\rm nodes}},R]}\|^2_{L^2} &\approx h \sum_{j=m(\varrho_{N_{\rm nodes}})}^{N-1} \left|\frac{u(r_{j+1}) - u(r_{j-1})}{2h}\right|^2 r_j^{d-1} \\ &\quad + \frac{(r_{m(\varrho_{N_{\rm nodes}})} - \varrho_{N_{\rm nodes}}) - h}{2} \left|\frac{u(r_{m(\varrho_{N_{\rm nodes}})+1}) - u(r_{m(\varrho_{N_{\rm nodes}})-1})}{2h}\right|^2 r_{m(\varrho_{N_{\rm nodes}})}^{d-1} \\ &\quad + \frac{r_{m(\varrho_{N_{\rm nodes}})} - \varrho_{N_{\rm nodes}}}{2} \left|\frac{u(r_{m(\varrho_{N_{\rm nodes}})}) - u(r_{m(\varrho_{N_{\rm nodes}})-1})}{h}\right|^2 \varrho_{N_{\rm nodes}}^{d-1} \\ &\quad + \frac{h}{2} \left|\frac{u(r_{N-1})}{2h}\right|^2 r_N^{d-1} \\ &:= \mathfrak{N}_{N_{\rm nodes}}(\boldsymbol{u}). \quad (16)\end{aligned}$$

For the case $k=0$, we use instead

$$\begin{aligned}\|\nabla u_{|[0,\rho_1]}\|_{L^2}^2 &\approx h\sum_{j=2}^{\ell(\varrho_1)}\left|\frac{u(r_{j+1})-u(r_{j-1})}{2h}\right|^2 r_j^{d-1}\\ &+\frac{(\varrho_1-r_{\ell(\varrho_1)})-h}{2}\left|\frac{u(r_{\ell(\varrho_1)+1})-u(r_{\ell(\varrho_1)-1})}{2h}\right|^2 r_{\ell(\varrho_1)}^{d-1}\\ &+\frac{\varrho_1-r_{\ell(\varrho_1)}}{2}\left|\frac{u(r_{\ell(\varrho_1)+1})-u(r_{\ell(\varrho_1)})}{h}\right|^2 \varrho_1^{d-1}\\ &:=\mathfrak{N}_0(\boldsymbol{u}).\end{aligned}\tag{17}$$

Thanks to (14) and (15)-(16)-(17), we can deduce an approximation of the projection $\Pi_{\mathcal{N}_{N_{\text{nodes}}}}$. By denoting $\mathfrak{E}_k(\boldsymbol{u})=\frac{1}{2}\mathfrak{N}_k(\boldsymbol{u})+\frac{1}{2}\mathfrak{L}_k^2(\boldsymbol{u})$, we obtain

$$\Pi_{\mathcal{N}_{N_{\text{nodes}}}}u\approx\mathfrak{P}_{N_{\text{nodes}}}\boldsymbol{u}:=\sum_{k=0}^{N_{\text{nodes}}}\boldsymbol{u}_{|\{m(\varrho_k),\ell(\varrho_{k+1})\}}\left(\frac{\mathfrak{E}_k(\boldsymbol{u})}{\mathfrak{L}_k^{p+1}(\boldsymbol{u})}\right)^{\frac{1}{p-1}},$$

where, for $1\leqslant j\leqslant N$,

$$\left(\boldsymbol{u}_{|\{m(\rho_k),\ell(\rho_{k+1})\}}\right)_j=\begin{cases}\boldsymbol{u}_j, & \text{if } m(\rho_k)\leqslant j\leqslant\ell(\rho_{k+1}),\\ 0, & \text{else.}\end{cases}$$

We can now gives a completely discretized version of the projected gradient descent method which is described in Algorithm 2 (where $[\boldsymbol{v}]_{i,j}=\boldsymbol{v}_j$ if $i=j$ and 0 if $i\neq j$).

Algorithm 2 The projected gradient descent method .

Require: $R,>0,\boldsymbol{u}^{(0)}\in\mathbb{R}^N,\tau>0,\varepsilon>0$
  Crit $\leftarrow 2\varepsilon$
  $j\leftarrow 0$
  while Crit $>\varepsilon$ **do**
    $\boldsymbol{v}\leftarrow(\mathrm{Id}-\tau([\Delta_{\mathrm{rad},R}]+[|\boldsymbol{u}^{(j)}|^{p-1}]))\boldsymbol{u}^{(j)}$
    $\boldsymbol{u}^{(j+1)}\leftarrow\mathfrak{P}_{N_{\text{nodes}}}\boldsymbol{v}$
    Crit $\leftarrow\max_{1\leqslant\ell\leqslant N}|\boldsymbol{u}_\ell^{(j+1)}-\boldsymbol{u}_\ell^{(j)}|$
    $j\leftarrow j+1$
  end while

5. Some properties of the Nehari and shooting methods

In this section, we discuss some properties of the methods that we have introduced. Our goal is to point out some of their strengths and weaknesses.

In the case of the shooting method, observe that there is an inherent numerical difficulty associated with its practical implementation. Indeed, given $k\in\mathbb{N}$, the value of α_k can be determined only up to machine precision, i.e. 10^{-16} in practice. This is limiting the size of the domain in x on which $u(\cdot;\alpha_k)$ can be computed accurately, even assuming no error on the numerical resolution of the Cauchy problem (10). Indeed, let $\varepsilon>0$ and define $w_\varepsilon=u(\cdot;\alpha_k)-u(\cdot;\alpha_k+\varepsilon)$. Then w_ε verifies

$$-w_\varepsilon''+w_\varepsilon-f'(u(\cdot;\alpha_k))w_\varepsilon=O(w_\varepsilon^2).$$

As $\lim_{r\to\infty}f'(u(r;\alpha_k))=0$, the linear part of the equation is given by $-w_\varepsilon''+w_\varepsilon$. Whenever w_ε become small enough so that $O(w_\varepsilon^2)$ becomes negligible, the

dynamics of the equation of w_ε becomes driven by the linear part, for which 0 is an exponentially unstable solution. As a consequence, we may have $w_\varepsilon(x) \sim \varepsilon e^x$, which leads to $w_\varepsilon \sim 1$ after $x \sim -\ln(\varepsilon)$ (after which nonlinear effects cannot be neglected any more). For $\varepsilon = 10^{-16}$, the best we can hope (assuming that the numerical method used to solve the ordinary differential equation is perfectly accurate) is therefore to solve our equation on an interval of length $-\ln(\varepsilon) \sim 36$. This is illustrated in Figure 2, on which we calculate the ground state with the shooting and Nehari methods in the case of the dimension $d = 2$ and for $p = 3$ when $R = 100$. We observe on the log-graph that at a distance from the origine around 19, the calculated solution starts to increase and goes far away from the expected solution (which is exponentially decreasing toward 0 at infinity). This issue is not observe in the case of the Nehari method due to the fact that we implement a Dirichlet boundary condition directly in the operator. This ensures that the numerical solution decreases properly to zero at the end of the domain.

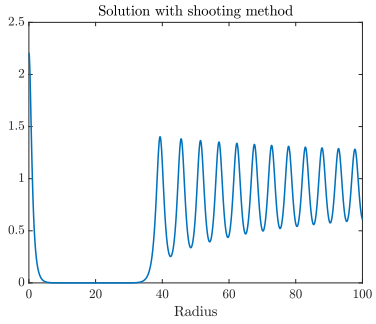

(A) Solution (shooting method)

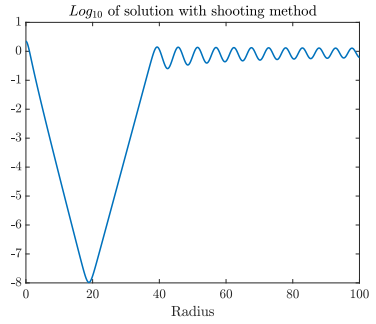

(B) Log_{10} of solution (shooting method)

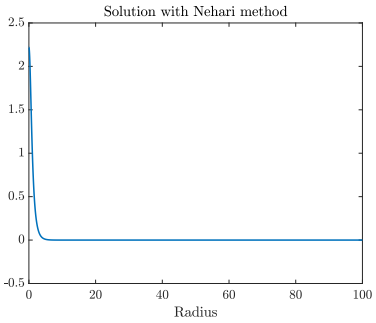

(C) Solution (Nehari method)

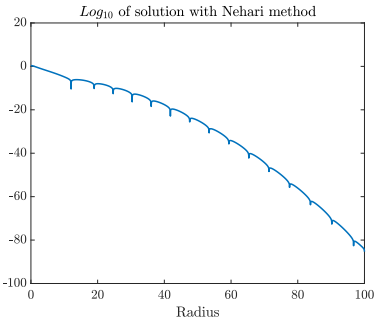

(D) Log_{10} of solution (Nehari method)

FIGURE 2. Computation of a ground state on large domain

We now turn to the number of iterations required to compute a bound state. In the case of the shooting method, this number is naturally bounded by the maximal number of iterations used in the dichotomy. With a maximal precision set to be $\varepsilon = 10^{-16}$ and an initial interval of length 100 for the initial data, the number of iterations will always be lower than $18 \log_2(10) \approx 60$. The Nehari method does not benefit from such bound on its number of iterations. In Figure 3, we depict the number of iterations necessary to the computation of bound states with respect to

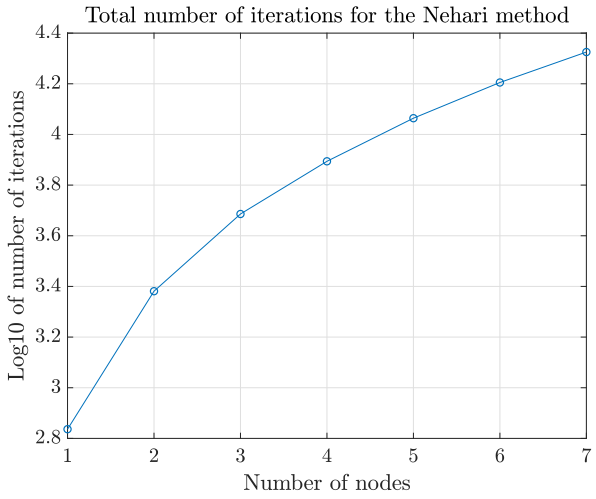

FIGURE 3. Total number of iterations for the Nehari method depending on the number of nodes

their number of nodes for $d = 2$, $p = 3$, $R = 30$ and $N = 2^{12}$. In each case, we use the following initial data

$$u_0(r) = \cos(r)e^{-r^2/30}.$$

We remark that this initial data has a large number of nodes and decreases rapidly to zero. By construction, the algorithm selects the desired number of nodes and the excess nodes are discarded. We can see that the number of iterations grows rapidly, making the Nehari method numerically costly compared to the shooting method.

Finally, we investigate the convergence properties of these methods with respect to the number of discretization points. To do so, we compute bounds states in dimension $d = 2$ and for $p = 3$ on the interval $[0, R]$, for $R = 30$, for different numbers of nodes with each method. The number of discretization points is set to be 2^N with $N \in \{8, 9, 10, 11, 12\}$ and we compute the errors

$$e_N^{(1)} := \|\boldsymbol{u}^{(N)} - \boldsymbol{u}^{(\mathrm{ref})}\|_{L^1} = h\sum_{k=1}^{2^N} |\boldsymbol{u}_k^{(N)} - \boldsymbol{u}_k^{(\mathrm{ref})}|$$
$$\text{and} \quad e_N^{(\infty)} := \|\boldsymbol{u}^{(N)} - \boldsymbol{u}^{(\mathrm{ref})}\|_{L^\infty} = \sup_{1\leqslant k\leqslant 2^N} |\boldsymbol{u}_k^{(N)} - \boldsymbol{u}_k^{(\mathrm{ref})}|,$$

for each N, where $\boldsymbol{u}^{(\mathrm{ref})}$ is the bound state computed with 2^{15} discretization points. The results are depicted in Figure 4 for the Nehari method and Figure 5 for the shooting method. We can see that the order of convergence of the Nehari method depends on the number of nodes and does not seems to be a specific value. However, we can affirm that it is of order above 1. In the case of the shooting method, the conclusion is more straightforward since the order of convergence is clearly 1 regardless of the number of nodes. This is explained by the fact that the positions of the nodes are computed with an error of the order of the space discretization.

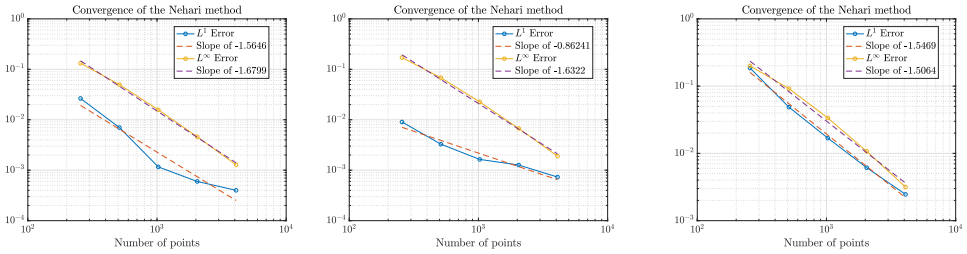

(A) $N_{\text{nodes}} = 1$ (B) $N_{\text{nodes}} = 2$ (C) $N_{\text{nodes}} = 5$

FIGURE 4. Convergence for the Nehari method depending on the number of nodes

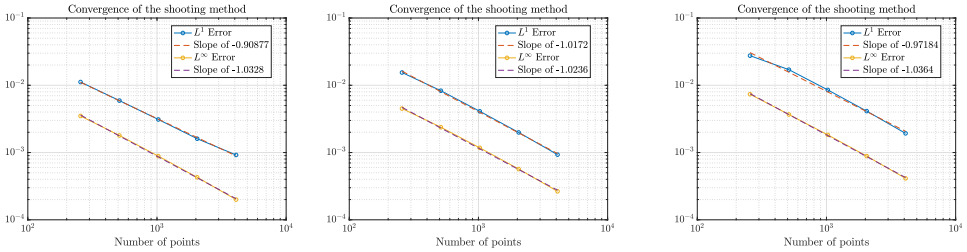

(A) $N_{\text{nodes}} = 1$ (B) $N_{\text{nodes}} = 2$ (C) $N_{\text{nodes}} = 5$

FIGURE 5. Convergence for the shooting method depending on the number of nodes

We then perform a comparison between the bound state obtained by each method in the same configuration. That is, we compute the errors

$$E_N^{(1)} := \|\boldsymbol{u}^{(N,\text{Nehari})} - \boldsymbol{u}^{(N,\text{Shooting})}\|_{L^1} = h \sum_{k=1}^{2^N} |\boldsymbol{u}_k^{(N,\text{Nehari})} - \boldsymbol{u}_k^{(N,\text{Shooting})}|$$

$$\text{and} \quad E_N^{(\infty)} := \|\boldsymbol{u}^{(N,\text{Nehari})} - \boldsymbol{u}^{(N,\text{Shooting})}\|_{L^\infty} = \sup_{1 \leqslant k \leqslant 2^N} |\boldsymbol{u}_k^{(N,\text{Nehari})} - \boldsymbol{u}_k^{(N,\text{Shooting})}|,$$

for each $N \in \{8, 9, 10, 11, 12\}$, where $\boldsymbol{u}^{(N,\text{Nehari})}$ (resp. $\boldsymbol{u}^{(N,\text{Shooting})}$) is the bound state obtained by the Nehari method (resp. the shooting method). The results can be observed in Figure 6 where we can see that, no matter the number of nodes, both methods converge to the same bound state.

In conclusion, we have studied two numerical methods to compute the bound states of the nonlinear Schrödinger equation in the radial case. The shooting method offers the advantage of being fast but the disadvantage of being less robust, whereas the Nehari method is robust but slow. Based on this observation, this suggest, for numerical experiments, to combine these two methods, that is, to make an initial approximation of the bound state using the shooting method and then refine it using the Nehari method to obtain the desired decay towards zero at infinity.

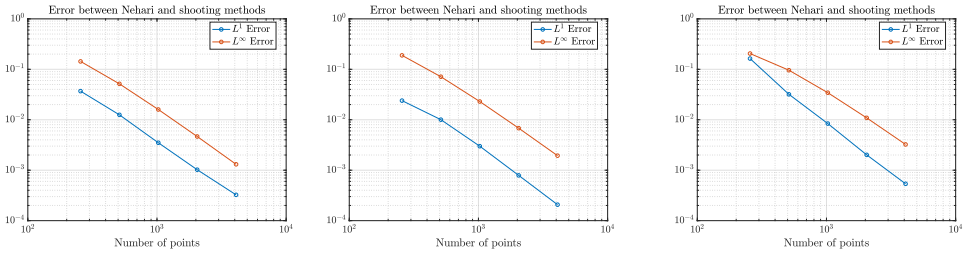

(A) $N_{\text{nodes}} = 1$ (B) $N_{\text{nodes}} = 2$ (C) $N_{\text{nodes}} = 5$

FIGURE 6. Gap between the bound states computed with the Nehari method and the shooting method

6. Numerical Experiments

In this section, we present some results obtained by numerical experiments consisting in running first the shooting method and then take the outcome as initial data for the Nehari method.

In Figure 7, we consider the case $d = 2$ and $p = 3$ and depict the relation between the number of nodes k of the bound state u_k and its initial value $u_k(0)$. We fit the data points with a function $k \mapsto a + b\sqrt{k}$ where $a = 0.4841$ (with 95 percent confidence bounds $[0.4487, 0.5194]$) and $b = 2.415$ (with 95 percent confidence bounds $[2.409, 2.422]$).

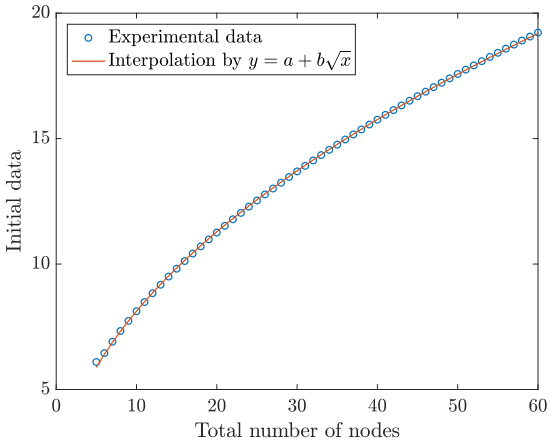

FIGURE 7. Evolution of the number of nodes depending on the value of the initial data

We also studied the positions of the nodes depending on the bound state (that is depending on its total number of nodes). These positions are depicted in Figure 8a. For each node, the position seems to follow a certain behavior that can be modeled by the function $k \mapsto 1/\sqrt{ak + b}$. We illustrate the value of the coefficients a and b for each node in Figure 8b.

In Figure 9, we plot the positions and (absolute) values of the extrema of the bound states between two consecutive nodes. We observe that for large numbers

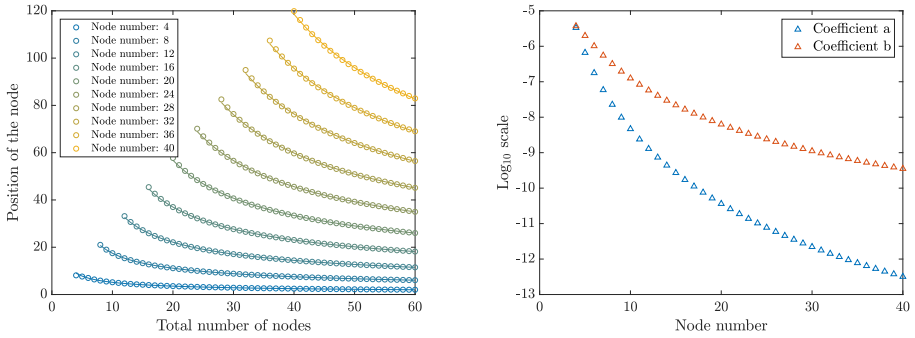

(A) Positions of the nodes (B) Interpolation's coefficients

FIGURE 8. Nodes positions and interpolation by $k \mapsto 1/\sqrt{ak+b}$

of nodes in the bound state, the extrema tend to a constant value which is $\sqrt{2}$. This can be explained by the fact that for large r the first derivative term in (9) vanishes and the solution is close to a soliton of the one dimensional setting whose expression is known to be $r \mapsto \sqrt{2}\,\mathrm{sech}(r)$. This is illustrated in Figure10 where we superimpose this soliton (adequately shifted) with the (absolute) value of the bound state between its last two nodes (with a total number of nodes equal to 60).

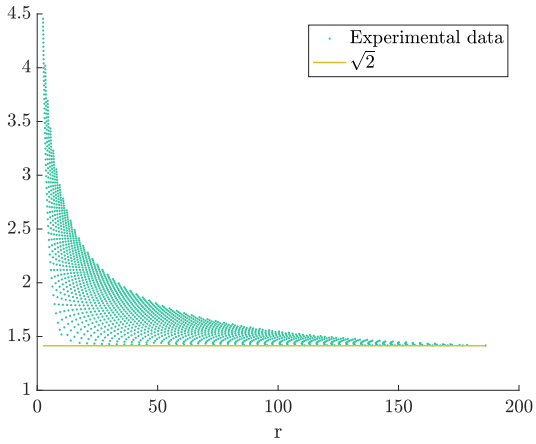

FIGURE 9. Local maxima of the bounds states by positions (x-axis) and values (y-axis)

APPENDIX A. QUANTITATIVE DEFORMATION LEMMA

In this appendix, we recall the quantitative Deformation Lemma used in the proof of Theorem 2.3.

For X in a Banach space and $S \subset X$, introduce the notation

$$S_\delta := \{u \in X | \operatorname{dist}(u, S) \leqslant \delta\},$$

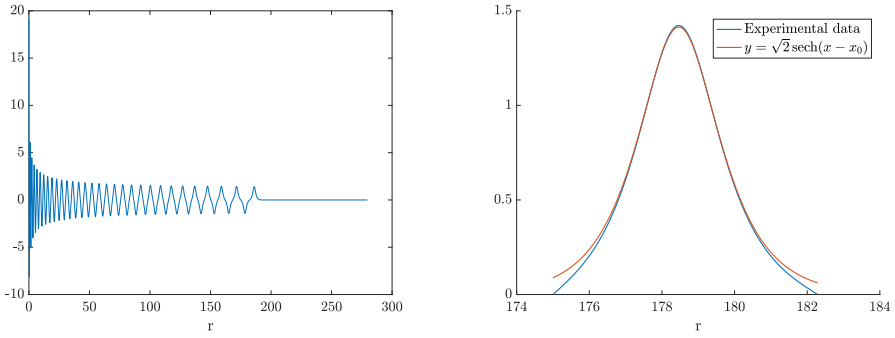

(A) The bound state (B) Final oscillation

FIGURE 10. Asymptotic behavior of the bound state with 60 nodes

and for $\varphi : X \to \mathbb{R}$, $c \in \mathbb{R}$, define

$$\varphi^c = \varphi^{-1}((-\infty, c]).$$

Lemma A.1 (Quantitative Deformation Lemma [26]). *Let X be a Banach space, $\varphi \in \mathcal{C}^1(X, \mathbb{R})$, $S \subset X$, $c \in \mathbb{R}$, $\varepsilon, \delta > 0$ such that*

$$\|\varphi'(u)\|_X \geqslant \frac{8\varepsilon}{\delta} \text{ for all } u \in \varphi^{-1}([c - 2\varepsilon, c + 2\varepsilon]) \cap S_{2\delta},$$

Then there exists $\eta \in \mathcal{C}([0, 1] \times X, X)$ such that

(i) $\eta(t, u) = u$ *if* $t = 0$ *or if* $u \notin \varphi^{-1}([c - 2\varepsilon, c + 2\varepsilon]) \cap S_{2\delta}$,
(ii) $\eta(1, \varphi^{c+\varepsilon} \cap S) \subset \varphi^{c-\varepsilon}$,
(iii) $\eta(t, \cdot)$ *is an homeomorphism of* X *for all* $t \in [0, 1]$,
(iv) $\|\eta(tu) - u\|_X \leqslant \delta$ *for all* $u \in X$ *and for all* $t \in [0, 1]$,
(v) $\varphi(\eta(\cdot, u))$ *is non increasing for all* $u \in X$,
(vi) $\varphi(\eta(t, u)) < c$ *for all* $u \in \varphi^c \cap S_\delta$ *and for all* $t \in (0, 1]$.

REFERENCES

[1] A. Ambrosetti and A. Malchiodi. *Perturbation methods and semilinear elliptic problems on* $\mathbb{R}^n$. Birkhäuser, Basel, 2006.
[2] A. Ambrosetti and A. Malchiodi. *Nonlinear analysis and semilinear elliptic problems*. Cambridge University Press, Cambridge, 2007.
[3] W. Ao, M. Musso, F. Pacard, and J. Wei. Solutions without any symmetry for semilinear elliptic problems. *J. Funct. Anal.*, 270(3):884–956, 2016.
[4] W. Bao and Q. Du. Computing the ground state solution of Bose-Einstein condensates by a normalized gradient flow. *SIAM J. Sci. Comput.*, 25(5):1674–1697, 2004.
[5] T. Bartsch and M. Willem. Infinitely many radial solutions of a semilinear elliptic problem on $\mathbf{R}^N$. *Arch. Rational Mech. Anal.*, 124(3):261–276, 1993.
[6] H. Berestycki, T. Gallouët, and O. Kavian. Équations de champs scalaires euclidiens non linéaires dans le plan. *C. R. Acad. Sci. Paris*, 297:307–310, 1983.
[7] H. Berestycki and P.-L. Lions. Nonlinear scalar field equations. I. Existence of a ground state. *Arch. Rational Mech. Anal.*, 82(4):313–345, 1983.
[8] H. Berestycki and P.-L. Lions. Nonlinear scalar field equations. II. Existence of infinitely many solutions. *Arch. Rational Mech. Anal.*, 82(4):347–375, 1983.
[9] C. Besse, R. Duboscq, and S. Le Coz. Gradient flow approach to the calculation of stationary states on nonlinear quantum graphs. *Ann. Henri Lebesgue*, 5:387–428, 2022.

[10] C. Besse, R. Duboscq, and S. Le Coz. Numerical simulations on nonlinear quantum graphs with the GraFiDi library. *SMAI J. Comput. Math.*, 8:1–47, 2022.
[11] D. Bonheure, V. Bouchez, C. Grumiau, and J. van Schaftingen. Asymptotics and symmetries of least energy nodal solutions of Lane-Emden problems with slow growth. *Commun. Contemp. Math.*, 10(4):609–631, 2008.
[12] T. Cazenave. *Semilinear Schrödinger equations*, volume 10 of *Courant Lecture Notes in Mathematics*. New York University / Courant Institute of Mathematical Sciences, New York, 2003.
[13] Y. S. Choi and P. J. McKenna. A mountain pass method for the numerical solution of semilinear elliptic problems. *Nonlinear Anal., Theory Methods Appl.*, 20(4):417–437, 1993.
[14] C. Cortázar, M. García-Huidobro, and C. S. Yarur. On the uniqueness of the second bound state solution of a semilinear equation. *Ann. Inst. H. Poincaré Anal. Non Linéaire*, 26(6):2091–2110, 2009.
[15] C. Cortázar, M. García-Huidobro, and C. S. Yarur. On the uniqueness of sign changing bound state solutions of a semilinear equation. *Ann. Inst. H. Poincaré Anal. Non Linéaire*, 28(4):599–621, 2011.
[16] D. G. Costa, Z. Ding, and J. M. Neuberger. A numerical investigation of sign-changing solutions to superlinear elliptic equations on symmetric domains. *J. Comput. Appl. Math.*, 131(1-2):299–319, 2001.
[17] G. Fibich. *The nonlinear Schrödinger equation*, volume 192 of *Applied Mathematical Sciences*. Springer, Cham, 2015.
[18] M. Ghimenti and J. Van Schaftingen. Nodal solutions for the Choquard equation. *J. Funct. Anal.*, 271(1):107–135, 2016.
[19] B. Gidas, W. M. Ni, and L. Nirenberg. Symmetry and related properties via the maximum principle. *Comm. Math. Phys.*, 68(3):209–243, 1979.
[20] M. K. Kwong. Uniqueness of positive solutions of $\Delta u - u + u^p = 0$ in $\mathbf{R}^n$. *Arch. Rational Mech. Anal.*, 105(3):243–266, 1989.
[21] P.-L. Lions. Solutions complexes d'équations elliptiques semilinéaires dans $\mathbf{R}^N$. *C. R. Acad. Sci. Paris Sér. I Math.*, 302(19):673–676, 1986.
[22] L. A. Maia, D. Raom, R. Ruviaro, and Y. D. Sobral. Mini-max algorithm via Pohozaev manifold. *Nonlinearity*, 34(1):642–668, 2021.
[23] W. A. Strauss. Existence of solitary waves in higher dimensions. *Comm. Math. Phys.*, 55(2):149–162, 1977.
[24] C. Sulem and P.-L. Sulem. *The nonlinear Schrödinger equation*, volume 139 of *Applied Mathematical Sciences*. Springer-Verlag, New York, 1999. Self-focusing and wave collapse.
[25] A. Szulkin and T. Weth. The method of Nehari manifold. In *Handbook of nonconvex analysis and applications*, pages 597–632. Int. Press, Somerville, MA, 2010.
[26] M. Willem. *Minimax theorems*. Progress in Nonlinear Differential Equations and their Applications, 24. Birkhäuser Boston, Inc., Boston, MA, 1996.

(Christophe Besse) Institut de Mathématiques de Toulouse ; UMR5219,
Université de Toulouse ; CNRS,
UPS IMT, F-31062 Toulouse Cedex 9,
France
Email address, Christophe Besse: christophe.besse@math.univ-toulouse.fr

(Romain Duboscq) Institut de Mathématiques de Toulouse ; UMR5219,
Université de Toulouse ; CNRS,
UPS IMT, F-31062 Toulouse Cedex 9,
France
Email address, Romain Duboscq: romain.duboscq@math.univ-toulouse.fr

(Stefan Le Coz) Institut de Mathématiques de Toulouse ; UMR5219,
Université de Toulouse ; CNRS,
UPS IMT, F-31062 Toulouse Cedex 9,
France
Email address, Stefan Le Coz: slecoz@math.univ-toulouse.fr